

Yi-Ling Hsieh¹
Tse-Hsien Chen¹
Ching-Piao Liu²
Chuen-Ying Liu¹

Titanium dioxide nanoparticles-coated column for capillary electrochromatographic separation of oligopeptides

¹Department of Chemistry,
National Taiwan University,
Taipei, Taiwan

²Department of Biochemical
Science and Technology,
National Taiwan University,
Taipei, Taiwan

A novel column made through the condensation reaction of TiO₂ nanoparticles (TiO₂ NPs) with silanol groups of the fused-silica capillary is described. EOF measurements under various buffer constitutions were used to monitor the completion of reactions. The results indicated that the EOF was dependent on the interactions between buffers and the bonded TiO₂ NPs. With formate/Tris buffer, EOF reversal at pH below 5 and cathodic EOF at pH above 5 were indicated. The pI of the bonded TiO₂ NPs was found at ~pH 5. Only cathodic EOF was illustrated by substituting the mobile phase with either glutamate or phosphate buffer. It was elucidated that both glutamate and phosphate buffer yield a negative charge layer on the surface of TiO₂ NPs attributable to the formation of a titanium complex. The CEC performance of the column was tested with angiotensin-type oligopeptides. Some parameters that would affect the retention behavior were investigated. The interactions between the bonded phases and the analytes were explicated by epitomized acid–base functional groups of the oligopeptides and the speciation of the surface oxide in different pH ranges. The average separation efficiencies of 3.1×10^4 plates/m is readily achieved with a column of 70 cm (50 cm) \times 50 μ m ID under an applied voltage of 15 kV, phosphate buffer (pH 6.0, 40 mM), and UV detection at 214 nm.

Keywords: Capillary electrochromatography / Condensation / Oligopeptides / Sol-gel / Stationary phase / Titanium dioxide nanoparticle
DOI 10.1002/elps.200500462

1 Introduction

Titanium dioxide has recently been drawing a great interest in the field of HPLC, due to the fact that it surpasses silica with regard to its hydrolytic stability. The surface of titanium dioxide was widely modified with octadecylsilane (ODS) for the comparison with traditional RP system [1–5]. In addition, Pinkse *et al.* [6] newly reported selected isolation at the femtomole level of phosphopeptides from proteolytic digests using 2-D-nanoLC-ESI-MS/MS and titanium oxide precolumns. A titanium dioxide precolumn has also been developed for selective adsorption of phosphopeptides by Sano and Nakamura [7]. However, little attention has been paid to the applicability of titanium dioxide in CE and CEC. A preliminary work concerning titanium dioxide coating

produced by the sol-gel method for CE separation of proteins was notified by Tsai *et al.* [8]. Fujimoto [9] prepared a titanium dioxide column by introducing a solution of titanium peroxo complex into the fused-silica capillary, followed by heating at an elevated temperature (450°C). He ascertained that satisfactory separation of four inorganic ions could be achieved, while an ODS-modified column was indispensable for the separation of carbohydrates and proteins.

The chemical and physical properties of a compound in nanosize are uniquely distinct from that in bulk material. Interaction phases in CEC normally consist of packed particles [10–13], monolithic beds [14–17], or bonded phases [18–24]. Recently, applications of nanoparticles as stationary phases of CEC have drawn attention. Gold particles in running buffer adsorbed to the capillary wall were consumed as interaction phases in open-tubular CEC [25]. The use of alkylthio gold nanoparticles in open-tubular CEC has been reported [26, 27]. Viberg *et al.* [28] employed polymeric nanoparticles as pseudostationary phases in CEC/ESI-MS for the separation of three amines. This technique shows promising features for analysis of analytes in complex matrixes, though it is not fully optimized for the separation.

Correspondence: Professor Chuen-Ying Liu, Department of Chemistry, National Taiwan University, 1, Sec. 4, Roosevelt Road, Taipei 10617, Taiwan
E-mail: cylieu@ntu.edu.tw
Fax: +886-2-23638543

Abbreviations: **Ang-I**, human angiotensin I acetate salt; **Ang-II**, human angiotensin II acetate salt; **Ang-ST**, [Sar¹, Thr⁸] angiotensin II acetate salt; **TiO₂ NPs**, TiO₂ nanoparticles; **TIP**, titanium (IV) isopropoxide

As a rule, peptides and proteins are separated by HPLC under gradient conditions. The substantial selection of sorbents for HPLC results from the extensively investigated separation mechanisms for peptides and proteins on these columns. As opposed to HPLC, CEC shows potential for the peptide separation attributable to its capabilities of separating charged and neutral molecules in a single run [29–32]. Yet, the stationary phases available for this new technique are under sprout. As long as more stationary phases are presented, CEC will be able to continue its rapid growth.

The aim of this work is to exploit TiO₂ nanoparticles (TiO₂ NPs) as the stationary phases of CEC. Based upon our experience, the open-tubular format is conceptually a simple column design in terms of CEC [18–23]. Nonetheless, a stable surface-bonded coating is essential to provide efficient chromatographic separations and reliable EOF. The column preparation by sol-gel approach is a proficient means since it enables a direct stationary phase bonding to capillary walls [33, 34]. Oliva *et al.* [35] studied the adsorption behavior of HSA onto colloidal TiO₂ particles. Therefore, the possibilities to prepare an open-tubular CEC column by condensation reaction from the TiO₂ NPs directly with the silanol groups on the surface of the inner wall of a fused-silica capillary are described. To characterize the prepared column further, angiotensin-type oligopeptides are employed as the model compounds to evaluate the separation performance.

2 Materials and methods

2.1 Apparatus

All experiments were carried out in a laboratory-built unit. It consists of a ± 30 kV high-voltage power supply (Gamma High Voltage Research, Ormond Beach, FL, USA) and a UV-visible detector (Model L-4200, Hitachi, Japan). Electrochromatograms were recorded and processed with a Peak-ABC Chromatography Workstation Ver. 2.11 (JiTeng Trading, Singapore) running on Window XP operating system. Fused-silica capillaries with 50 μ m ID and 375 μ m OD were purchased from Polymicro Technologies (Phoenix, AZ, USA).

2.2 Reagents and chemicals

Most chemicals were of analytical reagent grade from Merck (Darmstadt, Germany). Purified water (18 M Ω \times cm) from a Milli-Q water purification system (Millipore, Bedford, MA, USA) was used to prepare all solutions. Human angiotensin I acetate salt (Ang-I, pI 7.91), hu-

man angiotensin II acetate salt (Ang-II, pI 7.76), and [Sar¹, Thr⁸] angiotensin II acetate salt (Ang-ST, pI 9.85) were obtained from Sigma (St. Louis, MO, USA). Perchloric acid, benzyl alcohol, phosphoric acid, sodium phosphate (monobasic, dibasic, and tribasic) and Tris (Merck), formic acid, L-glutamic acid, 1-propanol, PEG (average $M_r = 8000$) (PEG 8000), sodium hydroxide and hydrochloric acid (Acros, Geel, Belgium), and titanium (IV) isopropoxide (TIP) (Fluka, Buchs, Switzerland) were purchased from the indicated sources.

Stock solutions of the oligopeptides (5 mg/mL) were prepared in pure water and diluted appropriately prior to use. All solvents and solutions for CEC analysis were filtered through a 0.45 μ m PTFE (Millipore) or cellulose acetate membrane (Whatman).

2.3 Sol-gel procedure

TiO₂ colloidal suspension was prepared by dropwise addition of 0.74 mL of 10% TIP in 1-propanol to perchloric acid solution (50 mL, pH 1.5) which was precooled at 4°C, with vigorous stirring in an ice bath for 1 h. The resultant mixture was further reacted at 50°C with stirring for 7 h. Freshly prepared colloidal suspension was used in all the experiments.

Transmission electron microscopy was carried out by applying 10 μ L of the colloidal sample to the carbon-coated copper grid. Particle sizes were determined from the photographs. Absorption spectra were recorded with a Hitachi U3200 spectrophotometer.

2.4 Column preparation

Fused-silica capillaries were first flushed with 1 M NaOH (30 min), then pure water (15 min), 1 M HCl (30 min), and pure water (15 min). Before introducing the sol-gel TiO₂ NPs, the capillaries were rinsed with methanol (5 min) and then dried in a GC oven at 110°C for 1 h under a nitrogen flow of 250 kg/m \times s².

PEG 8000 (16 mg) was added dropwise to the TiO₂ colloidal suspension (100 mL) with stirring to get a homogeneous solution, then concentrated under vacuum at 50°C to remove excess solvent (1-propanol). The resultant material (around 1 mL) was introduced into the capillary column under a nitrogen flow of 100 kg/m \times s² for 10 min, then plugged with GC septa and reacted at 150°C for 24 h. The resulting column was flushed successively with methanol, 0.1 M NaOH and pure water for 10 min to remove unreacted material.

2.5 Capillary electrochromatographic conditions

Before analysis, the coated capillaries were preconditioned with the running buffer. They were rinsed with methanol, pure water, and buffer between runs at 1 or 2 min intervals. The samples were injected electrokinetically. EOF was measured with benzyl alcohol. The samples were detected by UV light absorption measurement at 214 nm.

3 Results and discussion

3.1 Synthesis and characterization of the nanosized TiO₂ particles

TiO₂ colloidal suspensions are usually made by hydrolysis of alkoxide precursors in an aqueous acidic environment. In this work, it was prepared from the controlled hydrolysis of titanium (IV) isopropoxide (TIP) by following procedures in the literature [36].

3.1.1 Transmission electron micrographs

The transmission electron micrographs of the TIP hydrolysate are shown in Fig. 1. It clearly shows the colloidal suspension is homogeneous and the particle size is around 10 nm.

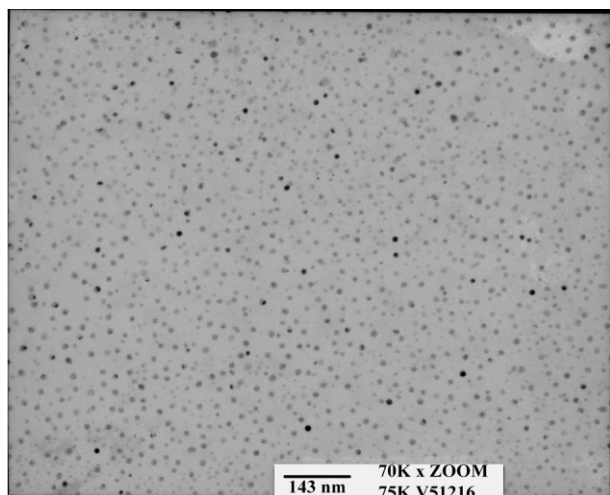


Figure 1. Transmission electron micrographs of TiO₂ NPs synthesized from the sol-gel method.

3.1.2 Absorption spectra

The UV spectrum shows the onset wavelength at 362 nm which is similar to that shown in [36]. This is evident for the formation of nanosized TiO₂ colloids. Since the reaction

rate for the hydrolysis of TIP is quite fast, TIP was diluted with 1-propanol prior to the reaction. A white precipitate was formed spontaneously at room temperature due to hydrolysis by the moisture in the air. For controlling the reaction rate, the sol-gel process was carried out at 4°C in an ice bath. The resultant product was transparent and colorless. To increase the yield, parameters which will affect the extent of hydrolysis and condensation reaction were studied. Increasing the temperature from 30 to 70°C and the duration up to 8 h, it was found that 50°C and an aging period of 7 h were the most favorable conditions for the nanoparticle preparation. The condition chosen was assayed by measuring the absorbance at 340 nm. If there is red-shift for the onset wavelength (362 nm) of the TiO₂ NPs, the absorbance at 340 nm will increase. A constant absorbance at 340 nm was recognized as accomplishment of the TIP hydrolysis. In this way, the prepared nanoparticles could be stable for more than 6 months. To produce a higher concentration of the product, the colloidal solution (100 mL) was concentrated under vacuum to remove isopropanol. The final volume was 1 mL, and the resulting concentration was around 40% w/v.

3.2 Column preparation

PEG 8000 was added to the TiO₂ colloidal (40% w/v) to avoid aggregation of the nanoparticles before introducing into the column [37]. The *pI* for sol-gel is defined as the pH where the zeta-potential is 0 [38]. The *pI* represents the point where electrostatic repulsion forces between colloidal particles are weakest, and, in most cases, the dispersion is most likely to aggregate [39]. To obtain and maintain a stable sol, peptization must generally be performed at a condition several pH units above or below the *pI*.

3.3 Characterization of the coated column

3.3.1 SEM picture of the coated capillary column

The size and morphology of the nanoparticles after introduced into the column was also determined with scanning electron microscope (SEM). For the sake of getting a thicker film thickness of the coated TiO₂ NPs, the column was initially prepared by one repetition coating procedures in Section 2.4. In other words, two condensation processes were carried out. Figure 2A indicates the cross section of the prepared column. It is evident that the inner surface of the capillary (50 μm ID) was covered by TiO₂ NPs. The coverage was nearly extended to the center of the column. Figure 2B is the magnification of the

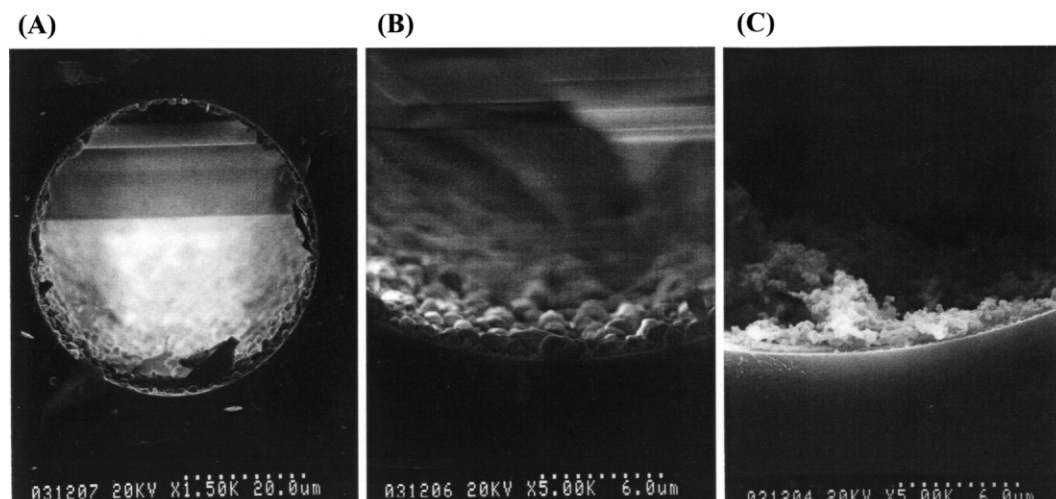


Figure 2. Scanning electron micrographs of TiO₂ NPs-coated column. (A) Cross section of the column prepared by two-cycle coating procedures. (B) Edge of the column prepared by two-cycle coating procedures. (C) Edge of the column prepared by a single coating procedure.

portion in Fig. 2A. It has been shown that TiO₂ NPs were tightly bonded onto the capillary column but the size of the microspheres is in the range from 10 to 100. Two condensation reactions might result in more aggregation of the nanoparticles. For comparison, only one condensation process was also carried out. Figure 2C shows the morphology of the resultant column. The nanoparticle size is distinctly smaller than that by one-repetition procedure (Fig. 2B).

3.3.2 Effect of buffer composition on the EOF

As shown in Fig. 3B, the buffer composition has a pronounced effect on the EOF of the coated capillary but it was not the case for bare fused silica (Fig. 3A). Here curves a, b, c designate phosphate buffer (pH 2–10), formate (pH 2–5)/Tris (pH 5–10), and glutamate buffer (pH 4–10), respectively. For a TiO₂ NPs-coated column, a reversal EOF was found at pH below 5 in the formate buffer. A positive charge on the surface of the column was indicated while at pH above 5, the direction of the EOF changed from anode to cathode. No signal could be found at pH around 5 regardless the marker was injected from the positive end or the negative end. It can be concluded that the pH might be exactly the *pI* of the coated material. The assumption was corresponding to that reported by Dobson *et al.* [40].

According to data shown in [35], the oxygen mono-coordinated titanium, pK_1 for $>Ti-OH_2^+ \rightarrow >Ti-OH + H^+$ is 2.60, pK_2 for $>Ti-OH \rightarrow >Ti-O^- + H^+$ is 9.00 while for oxygen di-coordinated titanium, the pK value for

$>Ti_2 = OH \rightarrow >Ti_2 = O^- + H^+$ is 5.50. It can be seen when the acidity of the medium is less than pH 4, the bridging group $>Ti_2OH$ was fully in the molecular form. The surface charge of the column mainly stemmed from the species of $>TiOH_2^+$. In this case, an EOF might be reversal. At pH over the range from 4 to 7, the terminal group on the coated material is $>TiOH$. The surface charge might originate from the dissociation of the bridging group $>Ti_2OH$ but at pH 4–5.5, only a little current was found. Much less surface charge is probably the reason, since its pK value is 5.50. At pH above 6, anodic EOF was switched into cathodic EOF due to the presence of highly dissociated $>Ti_2OH$. A buffer region was observed at pH around 9. This corresponds to the pK_2 value of the terminal $>TiOH$ group.

By changing the buffer composition into phosphate or glutamate buffer, only cathodic EOF was observed and no EOF reversal was indicated in the acidic solution. Phosphate ions are known to adsorb strongly to most metal oxides. It has been shown that phosphate ion binds to TiO₂ NPs as a bidentate surface species [41]. This resulted in a negative surface. The pK_a values for H₃PO₄ are 2.14, 7.19, and 12.30. As can be seen in Fig. 3B, two buffer regions were indicated. But the dissociation constants of the adsorbed phosphoric acid exhibited somewhat different values from those of the free phosphoric acid. The estimated pK_{a1} is 2.82 and pK_{a2} is 7.71.

Glutamic acid has two carboxylic acids and one amino group. The pK_a values are 2.10, 4.04, and 9.47. Surface-binding properties of carboxylic groups on nanoparticulate TiO₂ surface in hexanol has been studied by Weng *et*

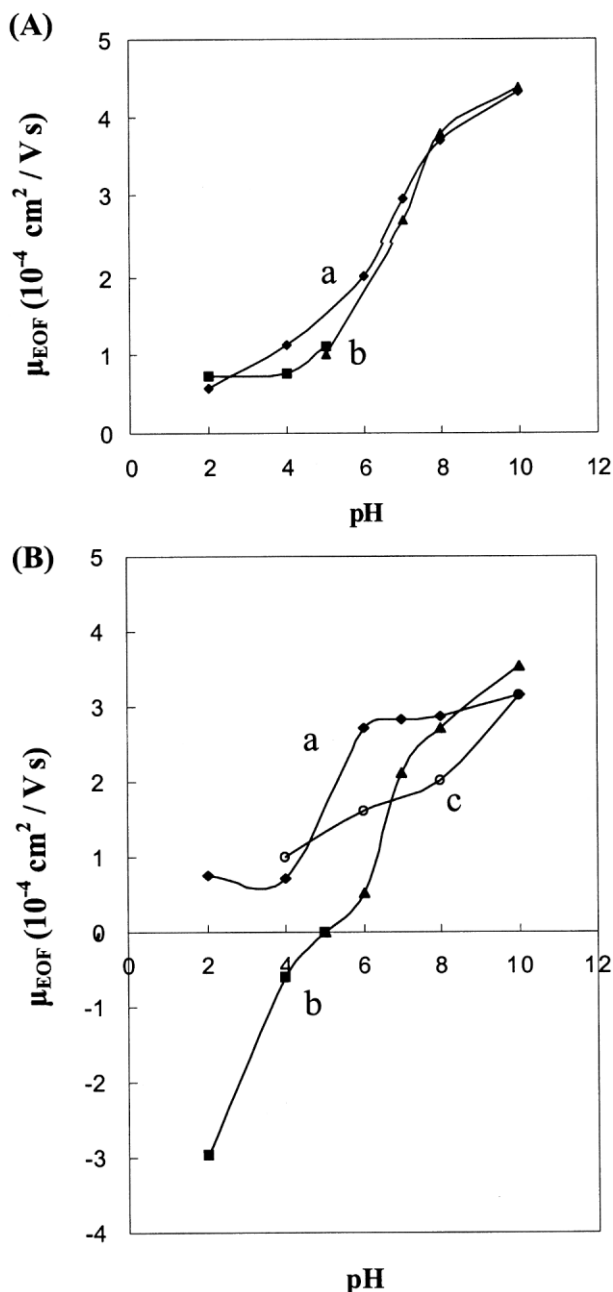


Figure 3. Effect of buffer pH and buffer composition on the EOF. Column dimension, 70 (50) cm \times 50 μm ID; injection, hydrodynamic method (10 cm, 2 s); marker, benzyl alcohol; voltage, +15 kV; detection, 214 nm. (A) Bare fused-silica column: (a) phosphate buffer (40 mM) and (b) formate/Tris buffer (40 mM). (B) TiO₂ NPs-coated column: (a) phosphate buffer (40 mM), (b) formate/Tris buffer (40 mM), and (c) glutamate buffer (40 mM).

al. [42]. They proposed that at pH 3, the main surface species on the nanoparticle is the ester-like linkage which constitutes about 63% of the total surface-binding molecules. The others are chelating and bridge forms as well

as hydrogen bonding and anion forms. Although the surface-binding forms of glutamate on nanoparticulate TiO₂ surface is not clear in our system, the cathodic EOF (Fig. 3B) indicates that a negative charge should be on the surface of TiO₂ NPs. In other words, glutamate molecules are really bonded onto the TiO₂ surface. Due to less variation among the pK_a values compared with phosphoric acid, a smooth curve was found for the plotting of EOF versus pH (Fig. 3B).

3.3.3 Effect of buffer concentration on EOF

At a phosphate concentration of 5 mM, the EOF was $1.5 \times 10^{-4} \text{ cm}^2 / \text{Vs}$. The dependence of EOF on phosphate concentration in the range from 10 to 50 mM was found to be nearly constant, $3 \times 10^{-4} \text{ cm}^2 / \text{Vs}$. The result indicated that 10 mM phosphate was enough for the coverage of the TiO₂ surface.

3.4 CEC separation of peptides

Here angiotensin-type peptides, Ang-ST, Ang-I, and Ang-II, were chosen as the model compounds.

3.4.1 Separation in formate/Tris buffer

At acidic condition of the formate buffer (pH 2, 40 mM), the EOF is reversal. The peptides carry the positive charge which migrated in the counter direction with the EOF. We can detect it in the cathode. This means that the mobility of peptides is greater than that of EOF. The elution order was Ang-I > Ang-ST > Ang-II (Figs. 4a–c). It was distinct at highly acidic condition (pH 2), and can be explained by the relative mobility shown in Table 1. Longer retention time was indicated for TiO₂ NPs column by comparison with that of the bare fused-silica column (Fig. 4), but no significant difference for the retention time on columns prepared via one- or two-cycle condensation processes. Only broadening and peak tailing were found for the latter treatment. No benefit was found for the repetition coating procedures. Hence, one condensation process was recommended for column preparation.

As stated before at formate/Tris buffer, the surface charge of the TiO₂ NPs is positive at pH below 5, while it carries negative charge at pH above 5. By further considering the pI values of these analytes, electrostatic attraction is responsible for the solute-bonded phase interaction at $5 < \text{pH} < 8$, while repulsive force was essential at the other outermost pH. Moreover, Ang-ST is the N-methylated sarcosine derivative of Ang-II. It is not easy to coordinate with the titanium ion. So it was eluted the earliest.

Table 1. Net charge and relative mobility of the analytes

| Analyte | Relative mobility ($\times 10^{-2}$) ^{a)} (net charge) ^{b)} | | | | | |
|---------------------------------|---|-------------|-------------|-------------|---------------|---------------|
| | pH 2 | pH 4 | pH 6 | pH 7 | pH 8 | pH 10 |
| Ang-I (M_r 1296.49; pI 7.91) | 3.09 (3.67) | 2.04 (2.42) | 0.85 (1.01) | 0.15 (0.18) | 0.00 (-0.01) | -0.98 (-1.17) |
| Ang-II (1046.19; 7.76) | 2.59 (2.67) | 1.39 (1.43) | 0.49 (0.51) | 0.09 (0.09) | -0.02 (-0.02) | -1.14 (-1.17) |
| Ang-ST (956.1; 9.85) | 2.77 (2.69) | 2.07 (2.01) | 1.55 (1.50) | 1.12 (1.09) | 1.01 (0.98) | -0.17 (-0.17) |

a) Relative mobility was calculated from the Offord's equation: $\mu_{rel} = \text{charge}/M_r^{2/3}$.

b) <http://www.embl-heidelberg.de/cgi-pi-wrapper.pl>

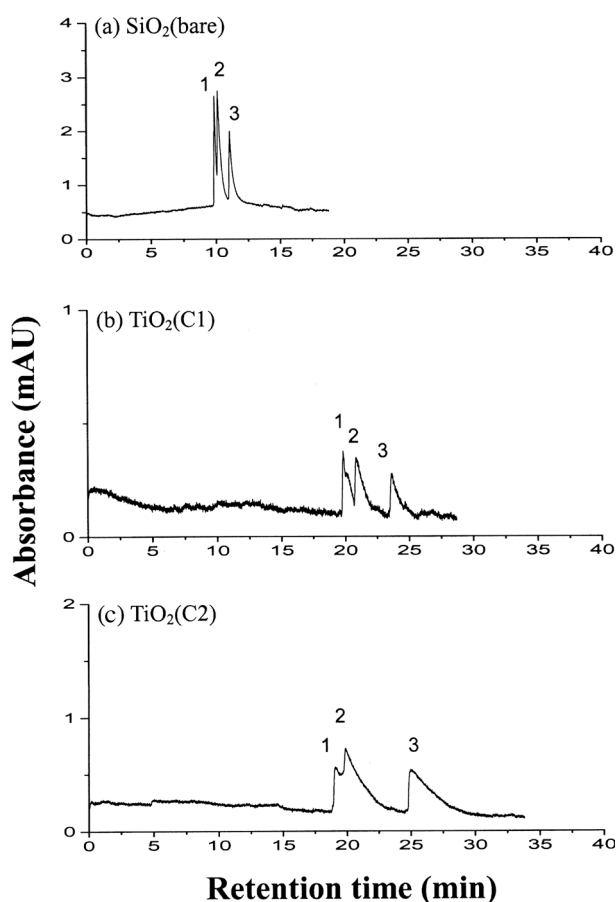


Figure 4. Film thickness of the TiO_2 NPs on the separation efficiency. Column dimension, 70 (50) cm \times 50 μm ID; sample concentration, 250 $\mu\text{g}/\text{mL}$ each; injection, 5 kV for 2 s; mobile phase, formate buffer (pH 2, 40 mM); voltage, +15 kV; detection at 214 nm. Peak identification: (1) Ang-I, (2) Ang-ST, and (3) Ang-II. (a) Bare fused silica. (b) TiO_2 NPs coated column (one-cycle coating). (c) TiO_2 NPs coated column (two-cycle coating).

Ang-I and Ang-II have aspartic acid in the *N*-terminal. A stable five-membered chelating ring with the titanyl ion would form. Because Ang-I has more amino acid residues

than Ang-II, greater steric hindrance for the complexation with the TiO_2 NPs might result in less affinity than Ang-II. Therefore, the elution order is Ang-ST > Ang-I > Ang-II. At pH below 6, a good separation was demonstrated (Fig. 5) but at pH above 7, the extent of ionization of both peptides and the surface negative charge of TiO_2 NPs increased. Charge repulsion increase resulted in lower affinity between them and eventually peak overlapping was observed.

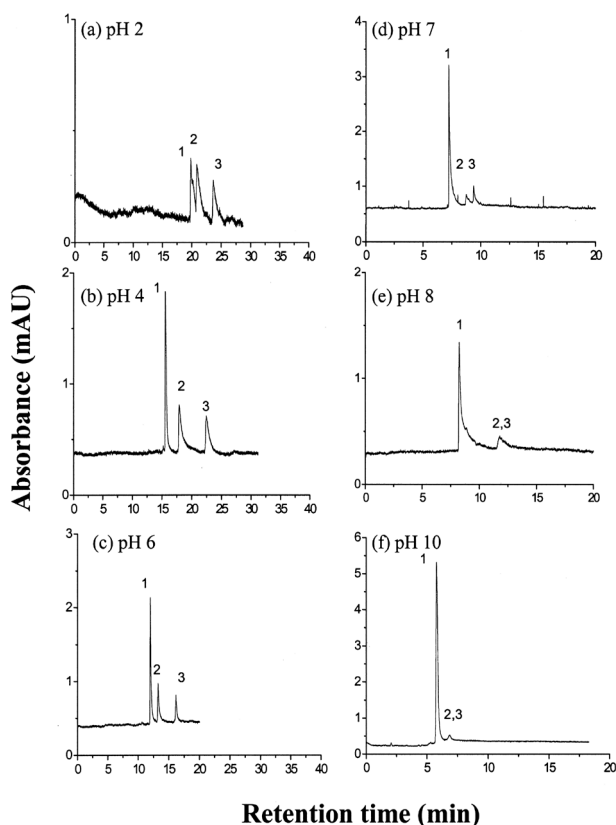


Figure 5. CEC separation of oligopeptides on TiO_2 NPs-coated column with formate/Tris buffer at various pH values. Conditions as in Fig. 4, except mobile phases (40 mM) are formate (pH 2–4) and Tris (pH 6–10). Peak identification: (1) Ang-ST, (2) Ang-I, and (3) Ang-II.

3.4.2 Separation in glutamate and phosphate buffer

In the EOF measurement, it was found that both glutamate and phosphate buffer yield a greater negative charge layer attributable to the formation of titanium complex. The analyte was coeluted with the EOF. Faster elution than that in the formate/Tris buffer was indicated (Figs. 6, 7). Additionally, better efficiency was demonstrated with phosphate buffer. One more evidence was given that phosphate has a greater ability than glutamate to displace the analytes coordinated with the TiO₂ NPs.

The influence of the phosphate buffer concentration (5, 10, 20, 40, and 50 mM) on separation was also examined. The higher the concentration, the greater peak height was indicated. On further increasing the concentration above 50 mM, slight peak tailing was demonstrated. This might be due to slower EOF mobility and Joule heating.

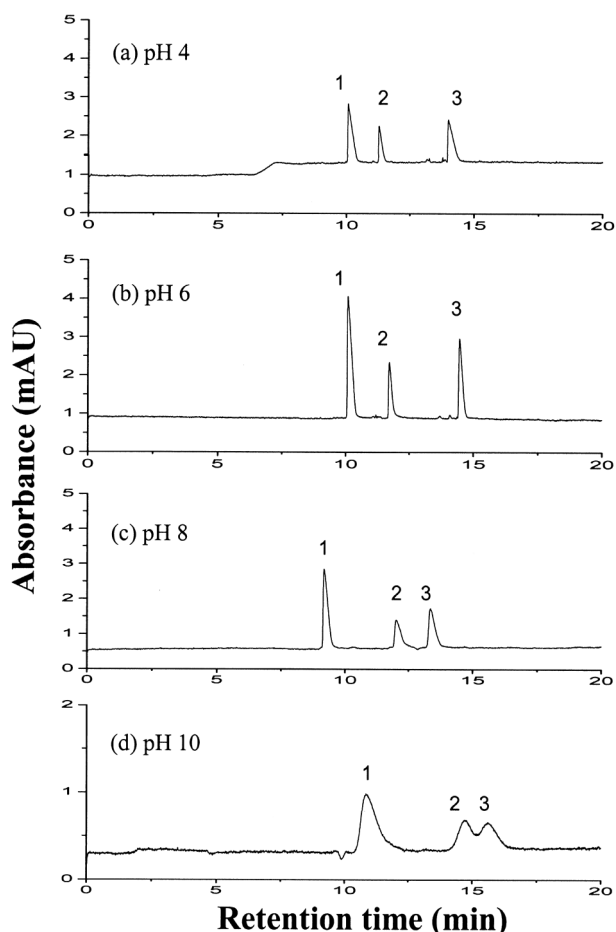


Figure 6. CEC separation of oligopeptides on TiO₂ NPs-coated column with glutamate buffer at various pH values. Conditions as in Fig. 4 except mobile phase: glutamate buffer (40 mM). Peak identification: (1) Ang-ST, (2) Ang-I, and (3) Ang-II.

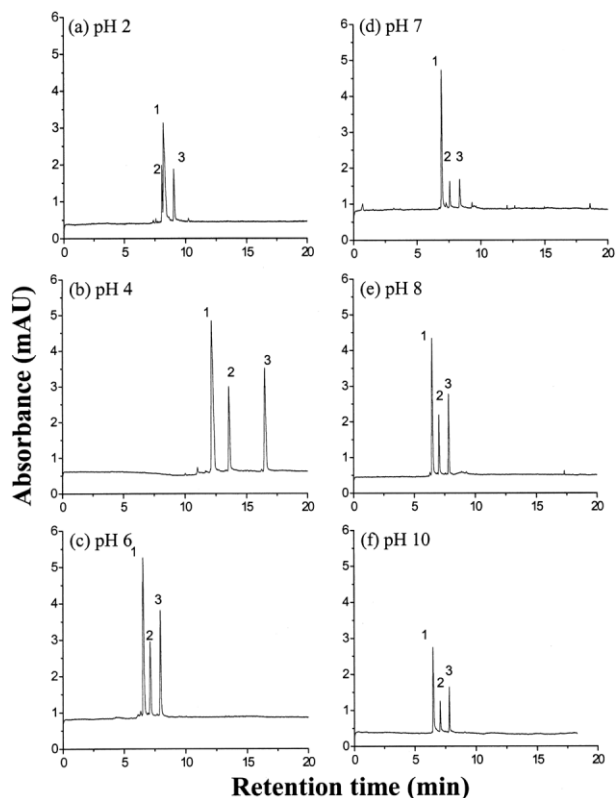


Figure 7. CEC separation of oligopeptides on TiO₂ NPs-coated column with phosphate buffer at various pH values. Conditions as in Fig. 4 except mobile phase: phosphate buffer (40 mM). Peak identification: (1) Ang-ST, (2) Ang-I, and (3) Ang-II.

3.5 Separation mechanism

The reactive groups in these peptides can be classified as follows: α -carboxyl, γ -carboxyl, imidazole, α -amino, ϵ -amino, methylamine, phenolic OH, and guanidyl. By considering the active groups of the analyte and the surface charge of TiO₂ NPs, ion-ion or ion-dipole, hydrogen bonding, and ligand exchange would be the main interaction force besides electrophoretic mobility difference. Since the coordination ability of the mobile phase with the TiO₂ NPs increased in the order: formate < Tris < glutamate < phosphate, the highest peak height along with the least elution time was expected with phosphate buffer (Fig. 7 compared with Figs. 5, 6).

3.6 Stability of the column

The separation efficiency for phosphate buffer is summarized in Table 2. With phosphate buffer (pH 6, 40 mM) and applied voltage of 15 kV, a good separation of the angio-

Table 2. Separation efficiency for the TiO₂ NPs-coated column^{a)}

| Analyte | pH 2 | | | pH 4 | | | pH 6 | | | pH 7 | | | pH 8 | | | pH 10 | | |
|---------|-------------|------------------------|---------------------|-------------|----------|-------|-------------|----------|-------|-------------|----------|-------|-------------|----------|-------|-------------|----------|-------|
| | t_R , min | N , /m ^{b)} | R_s ^{c)} | t_R , min | N , /m | R_s | t_R , min | N , /m | R_s | t_R , min | N , /m | R_s | t_R , min | N , /m | R_s | t_R , min | N , /m | R_s |
| Ang-ST | 8.21 | 98 000 | 0.7 | 12.18 | 26 000 | – | 6.56 | 22 000 | – | 6.94 | 38 000 | – | 6.46 | 29 000 | – | 6.51 | 40 000 | – |
| Ang-I | 8.06 | 16 000 | – | 13.58 | 83 000 | 2.4 | 7.15 | 32 000 | 3.5 | 7.58 | 52 000 | 3.1 | 7.04 | 56 000 | 3.9 | 7.09 | 63 000 | 5.4 |
| Ang-II | 9.04 | 53 000 | 2.9 | 16.48 | 81 000 | 1.6 | 7.69 | 40 000 | 4.0 | 8.37 | 40 000 | 2.3 | 7.83 | 40 000 | 2.5 | 7.83 | 94 000 | 3.8 |

a) TiO₂ NPs-coated column: 70 (50) cm × 50 μm; injection: 5 kV, 2 s; voltage: 15 kV; mobile phase: phosphate buffer (40 mM); detection at 214 nm

b) Theoretical plate: $N = 5.54 (t_R/w_{1/2})^2$, where t_R and $w_{1/2}$ represent the retention time and the peak width at half-maximum, respectively.

c) Resolution, $R_s = 2 (t_{R2} - t_{R1})/(W_1 + W_2)$.

tensin-type peptides could be achieved with average theoretical plates of 3.1×10^4 /m. The RSD for the retention time (min) was 1.21% for Ang-ST, 1.51% for Ang-I, and 1.43% for Ang-II based on five measurements between days. To assess the long-term stability of the column, the results from five consecutive injections were measured after the column had been used for longer than 1 month, namely, more than 100 injections have taken place. All RSD values were less than 3.00%. In this work, the procedure for the column preparation is very simple and convenient. The nanoparticles were introduced into the capillary under a nitrogen flow of 100 kg/m × s² lasting for 10 min. Therefore, it is easy to control the film thickness, which in turn is able to get highly reproducible column efficiency.

4 Concluding remarks

To our knowledge, this is the first attempt in CEC to use a simple way to prepare a titanium dioxide NPs-coated column. The covalent bonding was due to the condensation reaction directly with the silanol group on the inner wall of the fused-silica capillary. Dissimilar surface properties on the TiO₂ NPs were exhibited at formate/Tris, glutamate, and phosphate buffers. With angiotensin-type oligopeptides as model compounds, the separation performance indicated that the column could be highly promising for manipulation of the selectivity between solutes in CEC and other separation systems. Most of the stationary phases for the CEC separation of peptides or proteins are sol-gel/organic hybrid material irrespective the support is silica or titania [8, 9, 29–31, 33, 34]. Comparing the separation characteristics for a series of angiotensins on bare, diol-, and C-18-etched capillaries reported by Pesek *et al.* [29], the elution order is the same. But the column they used is made by the steps of etching, silanization, and organic moiety attaching. In this work,

only a TiO₂ NPs-coated column and no organic moiety attached was used for the separation of angiotensins. By considering the active groups of the analytes and the surface charge of TiO₂ NPs, ion-ion or ion-dipole, hydrogen bonding, and ligand exchange would be the main interaction force beside electrophoretic mobility difference. The separation of proteins will be described elsewhere.

The authors thank the National Science Council of Taiwan for financial support.

Received April 15, 2005

Revised August 3, 2005

Accepted August 3, 2005

5 References

- [1] Kawahara, M., Nakamura, H., Nakajima, T., *Anal. Sci.* 1989, 5, 763–764.
- [2] Trüdinger, U., Müller, G., Unger, K. K., *J. Chromatogr.* 1990, 535, 111–125.
- [3] Pesek, J. J., Matyska, M. T., Ramakrishnan, J., *Chromatographia* 1997, 44, 538–544.
- [4] Tani, K., Sumizawa, T., Watanabe, M., Tachibana, M., Koizumi, H., Kiba, T., *Chromatographia* 2002, 55, 33–37.
- [5] Jiang, Z. T., Zuo, Y. M., *Anal. Chem.* 2001, 73, 686–688.
- [6] Pinkse, M. W. H., Uitto, P. M., Hillhorst, M. J., Ooms, B., Heck, A. J. R., *Anal. Chem.* 2004, 76, 3935–3943.
- [7] Sano, A., Nakamura, H., *Anal. Sci.* 2004, 20, 861–864.
- [8] Tsai, P., Wu, C. T., Lee, C. S., *J. Chromatogr. B* 1994, 657, 285–290.
- [9] Fujimoto, C., *Electrophoresis* 2002, 23, 2929–2937.
- [10] Simal-Gándara, J., *Crit. Rev. Anal. Chem.* 2004, 34, 85–94.
- [11] Stol, R., Poppe, H., Kok, W. Th., *Anal. Chem.* 2003, 75, 5246–5253.
- [12] Piraino, S. M., Dorsey, J. G., *Anal. Chem.* 2003, 75, 4292–4296.
- [13] Chen, T. S., Liu, C. Y., *Electrophoresis* 2001, 22, 2606–2615.
- [14] Bedair, M., El Rassi, Z., *Electrophoresis* 2004, 25, 4110–4119.

- [15] Hilder, E. F., Svec, F., Fréchet, J. M. J., *J. Chromatogr. A* 2004, 1044, 3–22.
- [16] Chuang, S. C., Chang, C. Y., Liu, C. Y., *J. Chromatogr. A* 2004, 1044, 229–236.
- [17] Huang, Y. C., Lin, C. C., Liu, C. Y., *Electrophoresis* 2004, 25, 554–561.
- [18] Chen, G. J., Lee, N. M., Hu, C. C., Liu, C. Y., *J. Chromatogr. A* 1995, 699, 343–351.
- [19] Liu, C. Y., Chen, W. H., *J. Chromatogr. A* 1998, 815, 251–263.
- [20] Liu, C. Y., Ho, Y. W., Pai, Y. F., *J. Chromatogr. A* 2000, 897, 383–392.
- [21] Shiue, C. C., Lin, S. Y., Liu, C. Y., *J. Chin. Chem. Soc.* 2001, 48, 1029–1034.
- [22] Pai, Y. F., Liu, C. Y., *J. Chromatogr. A* 2002, 982, 293–301.
- [23] Lin, S. Y., Liu, C. Y., *Electrophoresis* 2003, 24, 2973–2982.
- [24] Guihen, E., Glennon, J. D., *J. Chromatogr. A* 2004, 1044, 67–81.
- [25] Neiman, B., Grushka, E., Lev, O., *Anal. Chem.* 2001, 73, 5220–5227.
- [26] O'Mahony, T., Owens, V. P., Murrphy, J. P., Guihen, E., Holmes, J. D., Glennon, J. D., *J. Chromatogr. A* 2003, 1004, 181–193.
- [27] Yang, L., Guihen, E., Holmes, J. D., Loughran, M., O'Sullivan, G. P., Glennon, J. D., *Anal. Chem.* 2005, 77, 1840–1846.
- [28] Viberg, P., Jornten-Karlsson, M., Petersson, P., Spégel, P., Nilsson, S., *Anal. Chem.* 2002, 74, 4595–4601.
- [29] Pesek, J. J., Matyska, M. T., Mauskar, L., *J. Chromatogr. A* 1997, 763, 307–314.
- [30] Pesek, J. J., Matyska, M. T., Dawson, G. B., Chen, J. I. C., Boysen, R. I., Hearn, M. T. W., *Anal. Chem.* 2004, 76, 23–30.
- [31] Matyska, M. T., Pesek, J. J., *J. Chromatogr. A* 2005, 1079, 366–371.
- [32] Unger, K. K., Hennessy, T. P., Huber, M., Hearn, M. T. W., Walhagen, K., *Anal. Chem.* 2002, 74, 200A–207A.
- [33] Malik, A., *Electrophoresis* 2002, 23, 3973–3992.
- [34] Li, W., Fries, D. P., Malik, A., *J. Chromatogr. A* 2004, 1044, 23–52.
- [35] Oliva, F. Y., Avalle, L. B., Cámara, O. R., de Pauli, C. P., *J. Colloid Interface Sci.* 2003, 261, 299–311.
- [36] Kamat, P. V., Flumiani, M., Dawson, A., *Colloids Surf. A* 2002, 202, 269–279.
- [37] Baraton, M. I., *Synthesis, Functionalization and Surface Treatment of Nanoparticles*, American Scientific Publishers, Stevenson Ranch, CA, 2003, Chapter 8.
- [38] Venz, P. A., Klopogge, J. T., Frost, R. L., *Langmuir* 2000, 16, 4962–4968.
- [39] Venz, P. A., Frost, R. L., Klopogge, J. T., *J. Non-Cryst. Solids* 2000, 276, 95–112.
- [40] Dobson, K. D., Connor, P. A., McQuillan, A. J., *Langmuir* 1997, 13, 2614–2616.
- [41] Connor, P. A., McQuillan, A. J., *Langmuir* 1999, 15, 2916–2921.
- [42] Weng, Y. X., Li, L., Liu, Y., Wang, L., Yang, G. Z., *J. Phys. Chem. B* 2003, 107, 4356–4363.